*Dynamics of Continuous, Discrete and Impulsive Systems*
*Series* **B:** *Applications & Algorithms* **31 (2024)** 321-337


# SELF-SIMILAR SOLUTIONS FOR A NEW FREE-BOUNDARY PROBLEM AND IMAGE CONTOUR ENHANCEMENT

Hossemddine Achour[1] Rafaa Chouder[2] and Noureddine Benhamidouche[3]

[1]Laboratory of Pure and Applied Mathematics,
University of M'sila, University Pole, Road Bourdj Bou Arreiridj, M'sila 28000 Algeria

[2]Laboratory of Pure and Applied Mathematics,
University of M'sila, University Pole, Road Bourdj Bou Arreiridj, M'sila 28000 Algeria

[3]Laboratory of Pure and Applied Mathematics,
University of M'sila, University Pole, Road Bourdj Bou Arreiridj, M'sila 28000 Algeria

**Abstract.** The nonlinear diffusion equation is used to analyze the process of edge enhancement in image processing, based on a new evolution model consider as a generalization of mean curvature motion. A free boundary problem is formulated describing the image intensity evolution in the boundary layers around the edges of image. An asymptotic self-similar solutions to this nonlinear diffusion equation are obtained in explicit forms. The solutions demonstrated that the edge enhancement and its rates depends on the parameters of equation. The experimental results demonstrate the effectiveness of the model in edge preservation.

**Keywords.** Nonlinear diffusion equations - Mean curvature motion - Total variation flow - Image enhancement - Free boundaries - Self-similar solutions.

**AMS (MOS) subject classification:** 35C06 - 35Q94 - 35R35 - 65M22 - 65N22.

# 1 Introduction

Many mathematicians have been attracted by image processing and computer vision in recent years. Methods based on partial differential equations (PDEs) have been extensively used. Thus, it is not surprising that many partial differential equations (PDEs) and variational approaches have contributed substantially to the mathematical foundations of signal and image analysis. The nonlinear diffusion equation is known to have a significant application in solving image processing issues. The use of diffusion equations for image processing was first initiated with the work of Perona and Malik [11], where the authors proved that image intensity flux can lead to image edge enhancement if the flux is directed opposite to the image intensity gradient. This was followed by a series of papers, starting with the one by Alvarez et

al. [1], they proposed a different approach to the edge enhancement problem. They selected the image flux direction orthogonal to the image intensity gradient. Malladi and Sethian [9, 10] proposed another model based on the differential-geometric approach. This model leads to the equation represents movement by curvature (curvature flow). Barenblatt and Vazquez in [2, 4], proposed to consider a more general flow given by the equation:

$$\partial_t u = \left(1 + |\nabla u|^2\right)^{\frac{1}{2}-\alpha} div\left(\frac{\nabla u}{\sqrt{1+|\nabla u|^2}}\right), \tag{1}$$

where $\alpha$ is a constant parameter, and can be written as:

$$\partial_t u = \frac{\left(1+u_y^2\right)u_{xx} - 2u_x u_y u_{xy} + \left(1+u_x^2\right)u_{yy}}{\left(1+u_x^2+u_y^2\right)^{1+\alpha}}, \tag{2}$$

where $u(x, y)$ is the image intensity and $x$ and $y$ are the Cartesian coordinates in the image plane, $t$ is time. Along with the former case $\alpha = 0$ (curvature flow), the case $\alpha = 1$ (Beltrami flow) has attracted the attention of researchers, cf. Sochen et al. [12].

The asymptotic and numerical treatment performed in the papers [12, 10] shows the enhancement of the intensity contrasts by the formation of regions of large intensity gradients. This phenomenon allowed Barenblatt in [2] to propose the existence of a boundary layer where large gradients concentrate and to focus on this boundary layer where a simplification of the model is possible. Using the Cartesian coordinates at the edge and choosing the $x$-axis as the direction normal to the boundary layer, the effect of the $y$ derivatives can be neglected with respect to the $x$ derivatives in (2). In this way, equation (2) in the boundary layer is reduced to its one-dimensional form:

$$\partial_t u = \frac{u_{xx}}{u_x^{2(1+\alpha)}}. \tag{3}$$

Authors in [2, 4] proposed a model for image contour enhancement where a free boundary problem has been formulated with equation (3). Their theory covers the existence and uniqueness solutions to the suitable problem, the existence and behaviour of bounding interfaces, and large-time behaviour. A self-similar solution is found for equation (3), for any $\alpha > 0$. Indeed it is constantly 0 or 1 outside a transition region (the grey zone) bounded by two curves, $l(t)$ and $r(t)$. The width of this transition region decreases with time, a token that the edge enhancement is taking place. Across the two delimiting curves, the intensity function $u$ is continuous, but its derivative $u_x$ suffers an infinite jump.

In the paper [7, 8] a travelling profile solutions are found for equation (3) for $\alpha > -\frac{1}{2}$, they also presented general results obtained for the free boundary problem.

In this paper, we consider a more general flow given by equation:

$$\partial_t u = \frac{1}{\left(1+|\nabla u|^2\right)^{\frac{q}{2}}} div\left(\frac{\nabla u}{\left(1+|\nabla u|^2\right)^{\frac{p}{2}}}\right), \tag{4}$$

which will be call the generalised mean curvature motion here. The constants $p$ and $q$ play the role of enhancement parameters. In other words, we study the following equation for image intensity:

$$\partial_t u = \frac{\left[u_y^2+(1-p)\,u_x^2\right]u_{xx} - 2pu_x u_y u_{xy} + \left[u_x^2+(1-p)\,u_y^2\right]u_{yy}}{\left(1+u_x^2+u_y^2\right)^{\frac{q}{2}+\frac{p}{2}+1}}, \tag{5}$$

we get the reduced equation, by further simplifications which is just the one-dimensional version of (5):

$$\partial_t u = (1-p)\,\frac{u_{xx}}{u_x^{(q+p)}}. \tag{6}$$

Equation (6) governs the evolution of the image intensity in the boundary layer. We can obtain the equation (3) for $p=0$ and $q=2\,(1+\alpha)$.

Our main goal in this work is to present different types of self-similar solutions for the free-boundary problem for equation (6) when the phenomenon of contour enhancement is taking place. To examine the validity of the theoretical results of equation (6) in 1-D, we present numerical simulations for the proposed model on 2-D Gray level images.

This paper is organized as follows; we present at first briefly a derivation of the classic intermediate asymptotic solution to the linear equation where exhibit no contour enhancement. Section (3) devoted to introducing a basic free-boundary problem to contour enhancement in one dimensional case. The next section is devoted to the presentation of different types of self-similar solutions for free-boundary problem when the phenomenon of contour enhancement is taking place. Section (5) briefly presents various numerical experiments. Finally the paper is ended by a short conclusion and some comments.

## 2 Intermediate-Asymptotic Solutions

In order to provide a useful comparison, we present at first briefly a derivation of the classic intermediate-asymptotic solution to the linear heat equation $u_t = (1-p)u_{xx}$ (formally corresponding to (6) for $q+p=0$ with $p<1$) for a "smoothed step" initial-boundary value problem:

$$u\,(x,0) = \begin{cases} 0, & -\infty < x \le -a_1 \\ u_0, & -a_1 \le x \le a_2 \\ 1, & a_2 \le x < +\infty \end{cases}, \tag{7}$$

with $a_1, a_2 > 0$ are constant parameters of the problem. We want to find a solution written in the form:

$$u(x,t) = \phi(\xi) \quad ,\xi = \frac{x - x_0}{a(t)}, \tag{8}$$

where $x_0$ is parameter to be fixed, and the profile $\phi(\xi)$ is an increasing function.
Substituting (8) into the linear heat equation. Easy integration under the boundary conditions $\phi(-\infty) = 0$, $\phi(+\infty) = 1$, allows one to obtain the function f in an explicit form

$$\phi(\xi) = \frac{1}{\pi} \int_{-\infty}^{\frac{\xi}{2\sqrt{1-p}}} e^{-\eta^2} d\eta, \tag{9}$$

offers the possibility to obtaining the function $u$ in an explicit form, and the solution can be expressed in terms of error function

$$u(x,t) = \frac{1}{2}\left[erf\left(\frac{x - x_0}{2(1-p)(t+A_0)^{\frac{1}{2}}}\right) + 1\right]. \tag{10}$$

Solution (10) demonstrates that the smoothed stepwise initial distribution extends with time; its properly defined width of the transition region increases with time proportionally to $\sqrt{t + A_0}$, and its gradient takes on a Gaussian space shape, $u_x(x,t) \sim t^{\frac{-1}{2}} e^{\frac{-x^2}{4t}}$, decreases with time and go to zero at $t \to \infty$ at a rate of the order of $t^{\frac{-1}{2}}$. (See Figure 1).

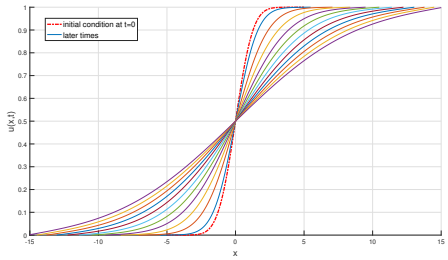


Figure 1: The evolution of the image intensity distribution $u(x,t)$ for heat equation.

Now we consider the nonlinear case defined by equation (6). We point out that, a series of numerical computations of the solutions to the suggested free-boundary problem for equation (6) for parameters $p$ and $q$ assumed the values $p = 0$ and $q = 4$, was performed in [2, 3]. The function $u_0(x)$ in some runs was non-monotonic. Computations demonstrated that the self-similar solution was an intermediate asymptotics of the solutions computed numerically. In [4], the same results obtained for a monotonic function $u(x)$. (See Figure 2).

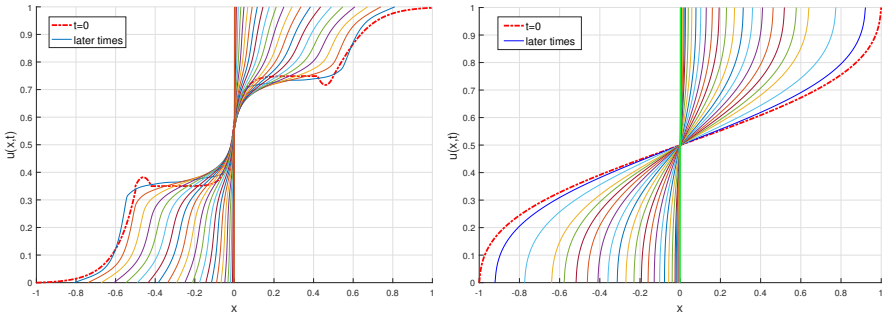


Figure 2: The evolution of the image intensity distribution for $p = 0$ and $q = 4$. left side, with non-monotonic initial condition. Right side, with monotonic initial condition.

We now address the main question of this paper, the construction of solutions with large gradients, appropriate for the contour enhancement problem.

# 3 Free boundary problem for contour enhancement

We introduce the following free boundary problem for determining the image intensity evolution in the boundary layer:
Given an increasing function $u_0(x)$ defined in an interval $I = (-a_1, a_2)$ with end values $u_0(-a_1) = 0$, $u_0(a_2) = 1$, to find a continuous function $u(x,t)$ and continuous curves $x = l(t)$ and $x = r(t)$ such that:

1. $l(0) = -a_1$, $r(0) = a_2$, and $l(t) < r(t)$ for some time interval $t \in (0, T)$.

2. $u$ solves the following problem in $\Omega = \{(x,t) : 0 < t < T,\ l(t) < x < r(t)\}$:

$$\begin{cases} \frac{\partial u}{\partial t} = (1-p)\, u_x^{-(q+p)} u_{xx}, & \text{in} \quad \Omega \\ u(x,0) = u_0(x), & \text{for} \quad -a_1 \le x \le a_2 \\ u(l(t),t) = 0, u_x(l(t),t) = +\infty & \text{for } 0 < t < T \\ u(r(t),t) = 1, u_x(r(t),t) = +\infty & \text{for } 0 < t < T \end{cases}, \tag{11}$$

for $q > 1-p$ and $p < 1$. $T$ can be finite or infinite time. The function $u(x,t)$ and the moving boundaries, $l(t)$ and $r(t)$, are unknowns, which must be determined by the over-specified conditions from the problem. This means that problem (11) is a free boundary problem. As a result, the interfaces $x = l(t)$ and $x = r(t)$ are also called " free-boundaries ". The initial conditions $u_0$ is monotone on the segment line $[-a_1, a_2]$ with $u_0(-a_1) = 0$, $u_0(a_2) = 1$. The solution $u(x,t)$ sharpens as $t$ grows; actually the two free boundaries

$l(t)$ and $r(t)$ shrink. If the two moving boundaries meet, a vertical front is formed, representing completed enhancement (see Figure 3).

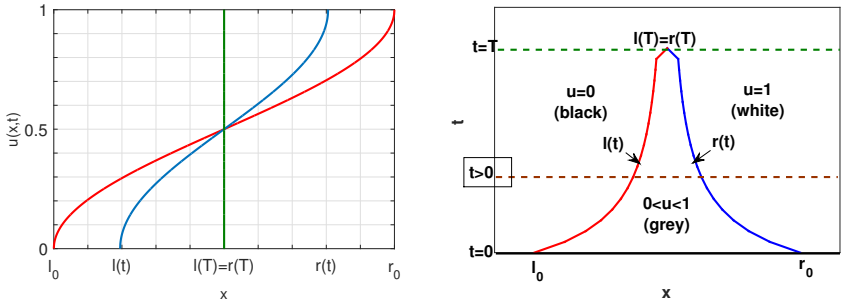


Figure 3: On the left, the front of the solution to the free boundary problem, respectively at time 0, and when complete enhancement occurs after some time $t$. On the right, the respective sections of the grey region, i.e. the transition domain.

A similar result (with possibly different rates) applies to more general values of parameters $1-p \geq q \geq -p$ with $p < 1$: they are purely diffusive and exhibit no contour enhancement (as we will see later). This yields to blurred results at the edges of image.

# 4 Self-similar solutions to the free boundary problem

We try now to solve problem (11) by using the self-similar solution under the form (8). Taking account this form, Substituting (8) into problem (11), we obtain, the equation:

$$-\frac{\dot{a}}{a}\xi\frac{d\phi}{d\xi} = (1-p)\,\frac{1}{a^{-(q+p)+2}}\frac{d^2\phi}{d\xi^2}\left(\frac{d\phi}{d\xi}\right)^{-(q+p)}, \quad \text{for } q > 1-p. \tag{12}$$

A separation of variables argument implies that the following conditions must hold :

$$\frac{\dot{a}}{a} = -\alpha\frac{1}{a^{-(q+p)+2}} \quad , \tag{13}$$

where $\alpha$ is arbitrary positive constant.
The equation for the profile $\phi$, becomes:

$$\alpha\xi\frac{d\phi}{d\xi} = (1-p)\,\frac{d^2\phi}{d\xi^2}\left(\frac{d\phi}{d\xi}\right)^{-(q+p)}.$$

After easy integration, we get:

$$\frac{d\phi}{d\xi} = \left[\frac{\alpha\,(q+p)}{2\,(1-p)}\right]^{\frac{-1}{q+p}} C^{\frac{-2}{q+p}} \left[1-\left(\frac{\xi}{C}\right)^2\right]^{\frac{-1}{q+p}}, \tag{14}$$

for

$$-C \le \xi \le C.$$

Here, $C$ is a positive integration constant. For $\xi = \frac{x-x_0}{a(t)}$, we have:

$$x_0 - Ca\,(t) \le x \le x_0 + Ca\,(t)\,.$$

The problem (11) suggests a free-boundary problem for determination of the image intensity evolution in the boundary layer $l\,(t)$ and $r\,(t)$ such that $l\,(t) \le x \le r\,(t)$, with $l\,(t) = x_0 - Ca\,(t)$ and $r\,(t) = x_0 + Ca\,(t)$.
The resolution of (13) gives,

$$a\,(t) = \left[\alpha\,(q+p-2)\,t + A_0\right]^{\frac{-1}{q+p-2}}, \quad \text{for } 0 < t < \infty \quad \text{if } q > 2-p, \tag{15}$$

and

$$a\,(t) = \left[\alpha\,(q+p-2)\,t + A_0\right]^{\frac{-1}{q+p-2}}, \quad \text{for } 0 < t < T \quad \text{if } 1-p < q < 2-p, \tag{16}$$

where $A_0 > 0$, is a constant, and $T$ is obtained as

$$T = -\frac{A_0}{\alpha\,(q+p-2)}.$$

In the particular case $q = 2-p$, we have:

$$a\,(t) = e^{-(1-p)\pi^2 t}, \qquad \text{for } 0 < t < \infty. \tag{17}$$

The value of the parameter $p$ and $q$ is important, so the different values of $p$ and $q$ lead to different behaviours of self-similar solutions, which is known as self-similar solutions of type I, for $q > 2-p$, type II for $1-p < q < 2-p$, in the case $q = 2-p$, we recover the self similar solutions of Type III .

According to the values of the parameters $p$ and $q$, we will discuss the asymptotic behaviours of self-similar solutions for (11), in order to study the phenomenon of contour enhancement.

Further integration of (14) and using the boundary conditions, implies $\phi\,(-C) = 0$, $\phi\,(C) = 1$, then we obtain:

$$\phi\,(\xi) = \left[\frac{\alpha\,(q+p)}{2\,(1-p)}\right]^{\frac{-1}{q+p}} C^{\frac{q+p-2}{q+p}} \int_{-1}^{\frac{\xi}{C}} \left[1-\eta^2\right]^{\frac{-1}{q+p}} d\eta,$$

where

$$C = \left[\frac{\alpha\,(q+p)}{2\,(1-p)}\right]^{-\frac{1}{q+p-2}} \left[2\int_0^1 \left[1-\eta^2\right]^{\frac{-1}{q+p}} d\eta\right]^{\frac{-(q+p)}{q+p-2}},$$

for $q \neq 2-p$.
The self-similar solution assumes the form

$$u(x,t) = \left[\frac{\alpha(q+p)}{2(1-p)}\right]^{\frac{-1}{q+p}} C^{\frac{q+p-2}{q+p}} \int_{-1}^{\frac{x-x_0}{Ca(t)}} \left[1-\eta^2\right]^{\frac{-1}{q+p}} d\eta, \tag{18}$$

and its gradient is given by

$$u_x = \frac{1}{a(t)} \left[\frac{\alpha(q+p)}{2(1-p)}\right]^{\frac{-1}{q+p}} C^{\frac{-2}{q+p}} \left[1-\left(\frac{x-x_0}{Ca(t)}\right)^2\right]^{\frac{-1}{q+p}}. \tag{19}$$

Relation (19) reveals important asymptotic properties of the image evolution in the boundary layer at the image edge. The width of the transition region $r(t) - l(t)$ equal to:

$$2Ca(t) = 2C\left[\alpha(q+p-2)t + A_0\right]^{\frac{-1}{q+p-2}}. \tag{20}$$

We discuss below the phenomenon of contour enhancement for different values of parameters $p$ and $q$.

## 4.1 Self-similar solution of type I

We start by studying the case $q > 2-p$ with $p < 1$. It is seen that, solution (18) is a local solution. At free boundaries $x = l(t)$ and $x = r(t)$, the image intensity is continuous but the derivative $u_x$ suffers an infinite jump. First of all, the width of the transition region (20), decreases with time, the step forms form an initially smoothed image $u_0$ and the edge enhancement takes place. Furthermore, the value of $u_x$ at $x = x_0$:

$$u_x(x_0,t) = \frac{1}{a(t)} \left[\frac{\alpha(q+p)}{2(1-p)}\right]^{\frac{-1}{q+p}} C^{\frac{-2}{q+p}},$$

is growing with time and blows up like "$O\left(t^{\frac{-1}{q+p-2}}\right)$" as $t \to \infty$. Therefore the validity of the asymptotic equation (6) improves with time.

The contour enhancement by evolution of image intensity function $u(x,t)$ illustrated in the Figure 4, we see that across the two delimiting curves the intensity function $u$ is continuous, but its derivative $u_x$ suffers an infinite jump. Moreover, the evolution arrives at a vertical front, so the enhancement happens.

## 4.2 Self-similar solution of type II

In contrast to solutions of type I which are defined globally in time, solutions of type II are exist only in a finite interval $0 < t < T$. We get this type for $1-p < q < 2-p$ with $p < 1$. The width of the transition region

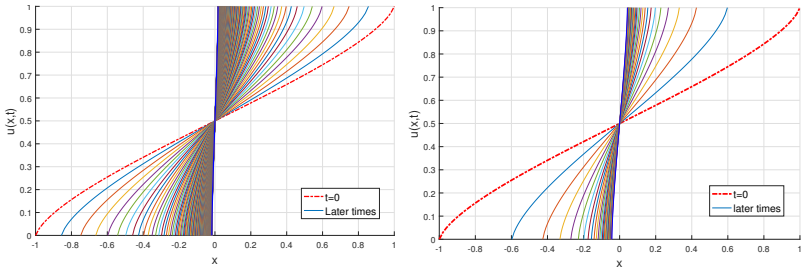


Figure 4: The evolution of the image intensity distribution $u(x,t)$. Top left: for $p=\frac{1}{2}$ and $q=\frac{5}{2}$. Top right : for $p=-1$ and $q=4$.

(20), decreases with time. In this case, a token that the edge enhancement is taking place: Across the two delimiting curves $(l(t), r(t))$, the intensity function $u$ is continuous, but its derivative $u_x$ suffers an infinite jump. The spatial gradient of the solution $u_x$ increases with time and blows up like "$O\left((T-t)^{\frac{-1}{q+p-2}}\right)$" as $t \to T$, its support shrinks. This leads to sharp edges in the image.

Figure 5 shows the self-similar solutions of problem (11) for different values of parameters $p$ and $q$ where $1-p<q<2-p$ with $p<1$. As mentioned above, the evolution is arrives at a vertical front in finite time.

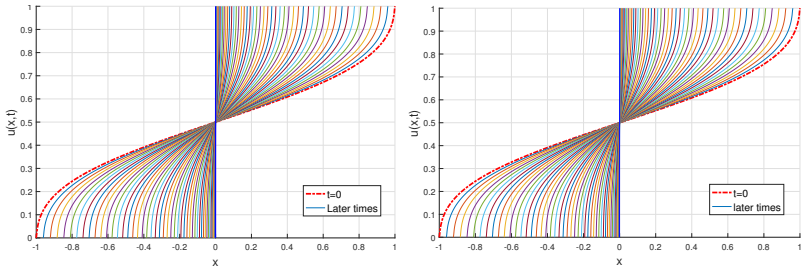


Figure 5: The evolution of the image intensity distribution $u(x,t)$. Top left : for value of $p=\frac{1}{2}$ and $q=1$. Top right : for value of $p=-1$, and $q=\frac{5}{2}$.

## 4.3 Self-similar solution of type III

Now, we study the special case $q=2-p$, with $p<1$. when we recover the self-similar solution of type III, The equation for the profile $\phi$ can be written as

$$\frac{d\phi}{d\xi}=\frac{1}{\pi C}\left[1-\left(\frac{\xi}{C}\right)^2\right]^{\frac{-1}{2}}, \tag{21}$$

for

$$-C \leq \xi \leq C.$$

Here, $C$ is an arbitrary positive integration constant. Further integration of (21) and using the boundary conditions, $\phi(-C) = 0$, $\phi(C) = 1$, then we obtain, the self-similar solutions of the Type III, assumes the form

$$u(x,t) = \frac{1}{\pi} \arcsin\left(\frac{x - x_0}{Ca(t)}\right) + \frac{1}{2}.$$

At free boundaries, the image intensity $u(x,t)$ is continuous. The gradient is given by

$$u_x = e^{(1-p)\pi^2 t} \frac{1}{\pi C} \left[1 - \left(\frac{x - x_0}{Ca(t)}\right)^2\right]^{\frac{-1}{2}}.$$

We remark that, for $q = 2-p$, the gradient blows up exponentially as $t \to \infty$. The width of the transition region $r(t) - l(t)$, which decreases with time. In this case the phenomenon of gradient enhancement takes place: The spatial gradient of the solution $u_x$, increases with time, and its support shrinks.

In this case the phenomenon of edge enhancement takes place, we notice that, the evolution arrives at a vertical front, so the enhancement happens after a larger time, (see Figure 6) .

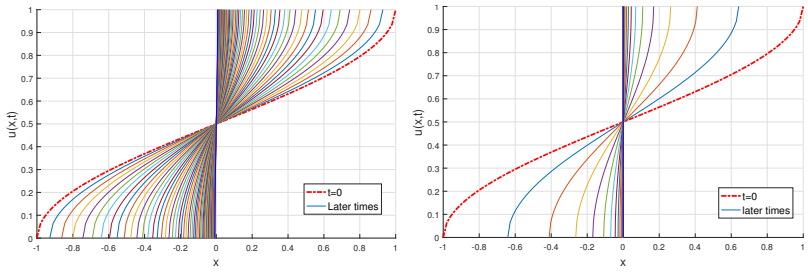


Figure 6: The evolution of the image intensity distribution $u(x,t)$. Top left : for value of $p = \frac{1}{2}$. Top right : for value of $p = -1$.

## 4.4 Non-enhanced contour for $1 - p \geq q \geq -p$

We now study the case where the enhancement does not occur, corresponding to the case of $1-p \geq q \geq -p$. The linear case studied in Section 2 corresponds to this case for $q = -p$. We try now to solve the equation in (11) by using the self-similar solution under the form (8). Taking account this form, by replacing (8) into equation (11), we obtain, the equation:

$$-\frac{\dot{a}}{a}\xi\frac{d\phi}{d\xi} = (1-p)\frac{1}{a^{-(q+p)+2}}\frac{d^2\phi}{d\xi^2}\left(\frac{d\phi}{d\xi}\right)^{-(q+p)}, \quad \text{for } 1-p \geq q > -p. \quad (22)$$

A separation of variables argument implies that the following conditions must hold :

$$\frac{\dot{a}}{a} = -\alpha \frac{1}{a^{-(q+p)+2}}, \tag{23}$$

where $\alpha < 0$ is arbitrary constant.
Easy integration gives:

$$a(t) = \left[\alpha (q+p-2) t + A_0\right]^{\frac{-1}{q+p-2}}, \qquad \text{for } \ 0 < t < \infty.$$

The equation for the profile $\phi$, becomes:

$$\alpha \xi \frac{d\phi}{d\xi} = (1-p) \frac{d^2\phi}{d\xi^2} \left(\frac{d\phi}{d\xi}\right)^{-(q+p)}. \tag{24}$$

After easy integration, we get:

$$\frac{d\phi}{d\xi} = \left[\frac{-\alpha (q+p)}{2(1-p)}\right]^{\frac{-1}{q+p}} C^{\frac{-2}{q+p}} \left[1 + \left(\frac{\xi}{C}\right)^2\right]^{\frac{-1}{q+p}}, \quad \text{for } 1-p \geq q > -p, \tag{25}$$

where

$$-\infty \leq \xi \leq +\infty.$$

By using the boundary condition $\phi(-\infty) = 0$, $\phi(+\infty) = 1$, we obtain, after integration:

$$\phi(\xi) = \left[\frac{-\alpha (q+p)}{2(1-p)}\right]^{\frac{-1}{q+p}} C^{\frac{q+p-2}{q+p}} \int_{-\infty}^{\frac{\xi}{C}} \left[1+\eta^2\right]^{\frac{-1}{q+p}} d\eta,$$

where

$$C = \left[\frac{-\alpha (q+p)}{2(1-p)}\right]^{-\frac{1}{q+p-2}} \left[2 \int_0^{\infty} \left[1+\eta^2\right]^{\frac{-1}{q+p}} d\eta\right]^{\frac{-(q+p)}{q+p-2}},$$

Thus, we obtain self-similar solutions, with the form

$$u(x,t) = \left[\frac{-\alpha (q+p)}{2(1-p)}\right]^{\frac{-1}{q+p}} C^{\frac{q+p-2}{q+p}} \int_{-\infty}^{\frac{x-x_0}{C a(t)}} \left[1+\eta^2\right]^{\frac{-1}{q+p}} d\eta. \tag{26}$$

We can see that, in this case $1-p \geq q > -p$ and $p < 1$, if $t \to \infty$, $u_x \to 0$.
For example when $q = 1-p$, the exact solution written under the form :

$$u(x,t) = \frac{1}{\pi} arctan\left(\frac{\alpha}{2\pi (1-p)} \frac{x-x_0}{t+A_0}\right) + \frac{1}{2}, \tag{27}$$

and its gradient is given by

$$u_x = \frac{\alpha}{2(1-p)(t+A_0)} \left[1 + \left(\frac{\alpha}{2\pi (1-p)} \frac{x-x_0}{t+A_0}\right)^2\right]^{-1}. \tag{28}$$

Solution (27) demonstrates the smoothed stepwise initial distribution extends with time; its properly defined width increases with time proportionally $(t + A_0)$, and its gradient (28) decreases with time and go to zero at $t \to \infty$ ( see Figure 7).

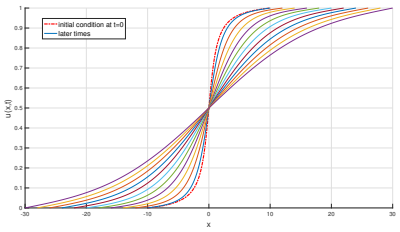


Figure 7: The evolution of the image intensity distribution for $q = 1 - p$.

# 5 Simulation Results for 2-D Gray Level Images

We now want to examine the validity of the theoretical results presented in the preceding sections for image enhancement. We will perform some numerical experiments on different types of images, such as gray-scale, to demonstrate the interest and efficiency of the proposed model (4). We will examine the efficiency of our model by performing some numerical experiments with different image types for certain values of the parameters $p$ and $q$, which correspond to the cases presented in the solutions of type I, type II, and type III.

For the numerical solution of equation (5) it is necessary to discretize the operators involved in the continuous problem.

We must approximate the first derivatives with respect to $x$ and $y$, the second derivatives with respect to $x$ and $y$, and the second cross derivative with respect to $x$ and $y$ in relation to spatial discretization. In fact, the following centering finite difference method can approximate the first derivative, the second derivative, and the second cross derivative, of the intensity $u$

$$\frac{\partial u}{\partial x} \approx \frac{u\left(x+h_x,y\right)-u\left(x-h_x,y\right)}{2h_x}+O\left(h_x^2\right),$$

$$\frac{\partial^2 u}{\partial x^2} \approx \frac{u\left(x+h_x,y\right)-2u\left(x,y\right)+u\left(x-h_x,y\right)}{h_x^2}+O\left(h_x^2\right),$$

$$\begin{aligned}\frac{\partial^2 u}{\partial x\partial y} \approx & \frac{u\left(x-h_x,y-h_y\right)-u\left(x-h_x,y+h_y\right)}{4h_xh_y} \\ & -\frac{u\left(x+h_x,y-h_y\right)-u\left(x+h_x,y+h_y\right)}{4h_xh_y}+O\left(h_x^2h_y^2\right).\end{aligned}$$

Let $\boldsymbol{A}$ be the spatial discretization matrix of problem (5). For the temporal discretization of problem (5) we can consider a semi-implicit scheme in time more convenient to implement. The solution of the time dependant problem

(5) by using an semi-implicit time marching scheme is defined by :

$$(Id + dt.A^q)\, U^{q+1} = U^q, \quad q = 1, 2, ...,$$

where $dt$ denotes the time discretization step, $Id$ is the identity matrix. At each time step we have to solve a large sparse algebraic system where the matrix $(Id + dt.A^q)$ is an irreducible strictly diagonal dominant matrix and then invertible, we can show that the semi-implicit time marching scheme is unconditionally stable. In the numerical processing, we will preferably use the semi-implicit time marching scheme, due mainly to the convenience of using this numerical scheme.

### 5.1 Numerical experiments and discussion

Now we show some numerical examples to illustrate the behaviour of equation in 2-D and compare them with the reduced equation in 1-D for different values of $q$ and $p$.

Figures 8 to 12, illustrate the results of the application of equation (5) to 2-D gray level images. By comparing between the images, display the results obtained by using different values of parameters $p$ and $q$ for a large stopping time and the evolution of equation (6) corresponding.

In Figure 8 we can see that the linear filter has blurred edges after a number of steps. In contrast, in figure 8(a) dot-dash correspond the image original (initial condition), the width of the transition region $r\,(t) - l\,(t)$ which increases with time, this yields to blurred results at the edges of image.

A similar result with the linear case, for $q = 1 - p$, we see that in Figure 9 this yields to blurred results at the edges of image with large time.

On the other hand, Figures 10 to 12, shows the results of the application to the same test image. We see that the values of $q > 1 - p$ has done a superior job of preserving edges even for a larger stopping, leads to sharp edges and enhancement image. It also can be observed from the 1-D , the curves are parametrized by time, evolving with increasing $t$ towards the sharp front, the width of the transition region decreases with time, the spatial gradient of the solution $u_x$, increases with time, so the edge enhancement takes place.

Our numerical experience which is also confirm the self-similar approach is valid for the study of contour enhancement.

## 6 Conclusion

We have established the asymptotic analysis of a free boundary problem that represents a one-dimensional version of a new model consider as a generalization of mean curvature motion. This problem formulated for the image intensity evolution in the boundary layer around the edge of image. Analysis of self-similar solutions for the image evolution in the boundary layer demonstrated that the edge enhancement and its rates depends on the parameters

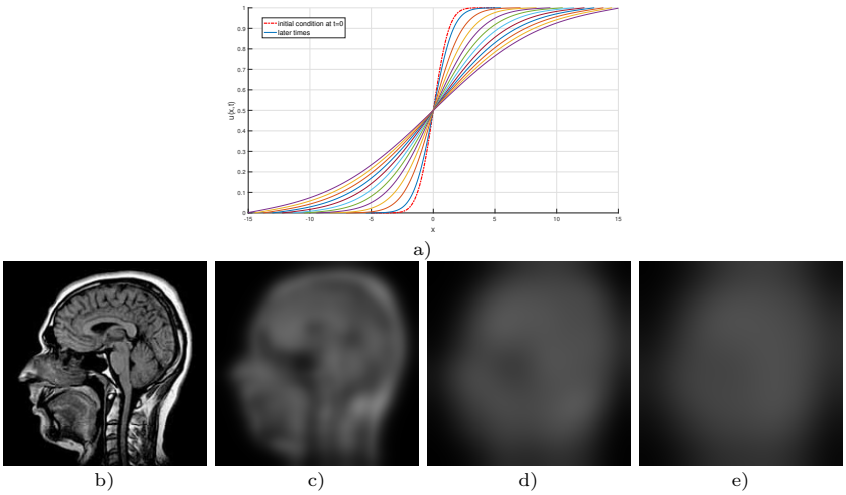


Figure 8: Comparison of the evolution of the image intensity distribution in 1-D (heat eqution) for $p = q = 0$, and the evolution of equation in 2-D (5). The first row corresponds the evolution of the image intensity in 1D. Second row shows the initial image and results with image filtred after (20,50,100) iteration, the resulting image is blurred.

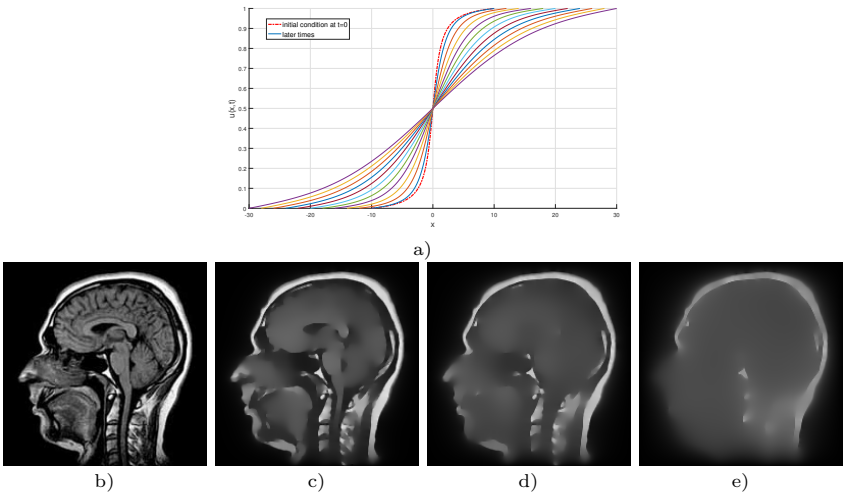


Figure 9: Comparison of the evolution of the image intensity for the special case $q = 1-p$ in 1-D, and the evolution of equation corresponding in 2-D (5). For $p = \frac{1}{2}$ and $q = \frac{1}{2}$, the first row shows the evolutio in 1-D. Second row corresponds the initial image and results with image filtred after (50,100,200) iteration, the resulting image is blurred.

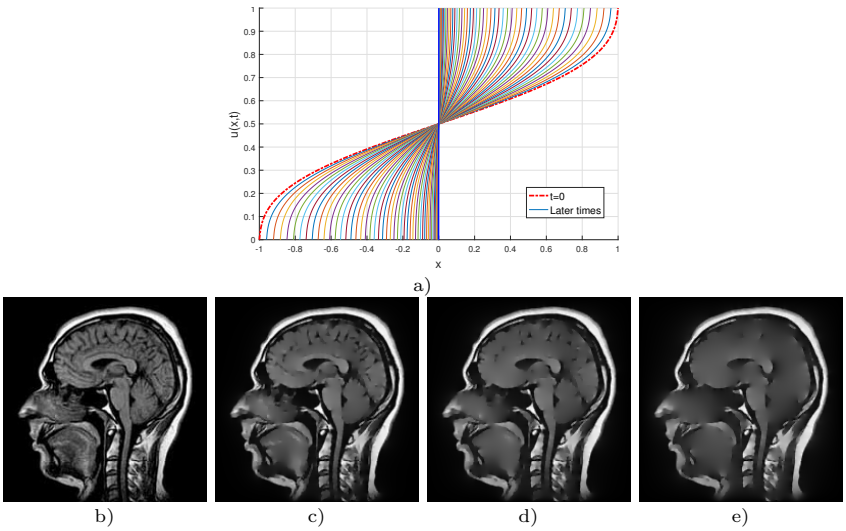


Figure 10: Comparison of the evolution of the image intensity distribution corresponding in 1-D i the case $1-p<q<2-p$ (type II), and the evolution of equation corresponding in 2-D (5). For $p=\frac{1}{2}$ and $q=1$, the first row the evolution in 1D. Second row shows the initial image and results with image filtred after (50,100,200) iteration.

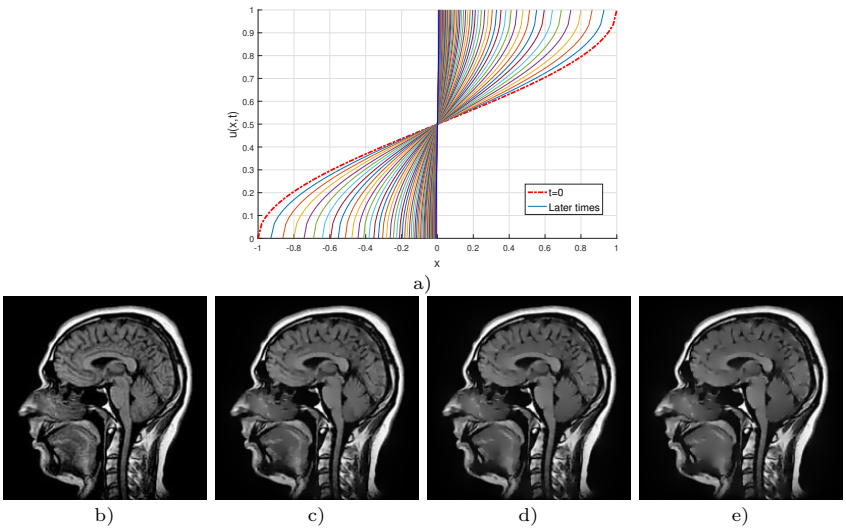


Figure 11: Comparison of the evolution of the image intensity distribution corresponding in 1-D in the case $q=2-p$ (type III), and the evolution of equation corresponding in 2-D (5). For $p=\frac{1}{2}$ and $q=\frac{3}{2}$, the first row the evolution in 1D. Second row shows the initial image and results with image filtred after (50,100,200) iteration.

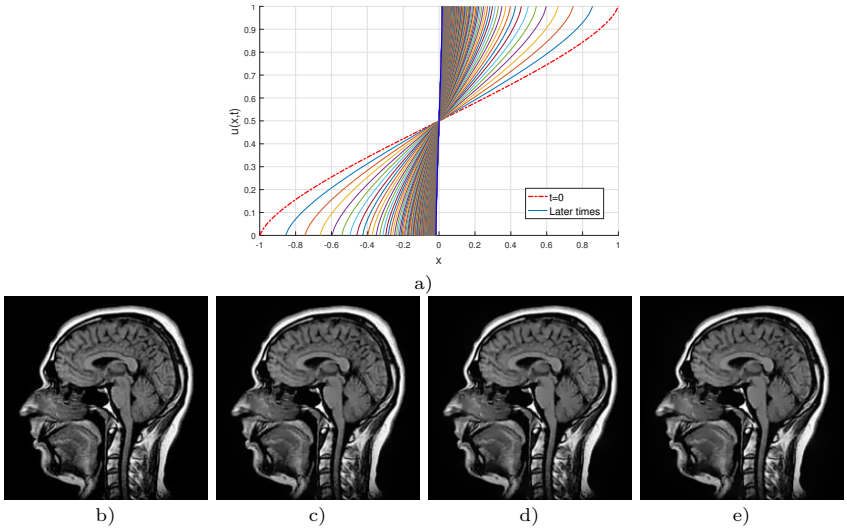


Figure 12: Comparison of the evolution of the image intensity distribution corresponding in 1-D in the case $q > 2 - p$ (type I), and the evolution of equation corresponding in 2-D (5). For $p = \frac{1}{2}$ and $q = \frac{5}{2}$, the first row the evolution in 1D. Second row shows the initial image and results with image filtred after (50,100,200) iteration.

$p$ and $q$. We can agree closely that our model leads to obtaining satisfactory results about image enhancement. According to the numerical simulations in 2-D, which proved that the proposed model is more efficient because is operates on the preserving of contour.

## Acknowledgments

This research work is supported by the The General Direction of Scientific Research and Technological Development (DGRSDT)- Algeria.

## Conflict of interest

On behalf of all authors, the corresponding author stetes that there is no conflict of interest.

# References

[1] L. Alvarez, P.L. Lions and J.M. Morel, Image selective smoothing and edge detection by nonlinear diffusion II, *SIAM Journal on Numerical Analysis*, **29**, (1992) 845-866.

[2] G.I. Barenblatt, Self-similar intermediate asymptotics for nonlinear degenerate parabolic free-boundary problems that occur in image processing, *Proceedings of the National Academy of Sciences of the United States of America*, **98**, (2001) 12878-12881.

[3] G.I. Barenblatt M. Bertsch, A.E. Chertock, and V.M. Prostokishin, Self-similar intermediate asymptotics for a degenerate parabolic filtration-absorption equation, *Proceedings of the National Academy of Sciences of the United States of America*, **97**, (2000) 9844-9848.

[4] G.I. Barenblatt and J.L. Vázquez, Nonlinear diffusion and image contour enhancement, *Interfaces and Free Boundaries*, **6**, (2003) 31-54.

[5] B. Basti and N. Benhamidouche, Global existence and blow-up of generalized self-similar solutions to nonlinear degenerate diffusion equation not in divergence form, *Applied Mathematics E-Notes*, **20**, (2020) 367-387.

[6] N. Benhamidouche, Exact solutions to some nonlinear PDEs, travelling profiles method, *Electronic Journal of Qualitative Theory of Differential Equation*, **15**, (2008) 1-7.

[7] R. Chouder and N. Benhamidouche, New exact solutions to nonlinear diffusion equation that occurs in image processing, *International Journal of Computing Science and Mathematics*, **10**, (2019) 364-374.

[8] R. Chouder and N. Benhamidouche, Travelling profile solutions for nonlinear degenerate parabolic equation and contour enhancement in image processing, *Applied Mathematics E-Notes*, **18**, (2018) 1-12.

[9] R. Malladi and J.A. Sethian, Image processing via level set curvature flow, *Proceedings of the National Academy of Sciences*, **92**, (1995) 7046-7050.

[10] R. Malladi and J.A. Sethian, Image Processing: Flows under Min/ Max curvature and mean curvature, *Graphical Models and Image Processing*, **58**, (1996) 127-141.

[11] P. Perona and J. Malik, Scale-space and edge detection using anisotropic diffusion, *IEEE Transactions on Pattern Analysis and Machine Intelligence*, **12**, (1990) 629-639.

[12] N. Sochen, R. Kimmel and R. Malladi, From high energy physics to low level vision, *International Conference on Scale-Space Theories in Computer Vision*, (1997) 236-247.

email: journal@monotone.uwaterloo.ca
http://monotone.uwaterloo.ca/∼journal/